Three-dimensional organization of the *pars fibroreticularis* framework of the urethral wall in normal human prostates

Jorge H.M. Manaia, Gilberto P. Cardoso, Lucas A.S. Pires, Marcio A. Babinski

Fluminense Federal University, Niterói, Brazil

Corresponding author:
Marcio A. Babinski PhD
Fluminense Federal University
Av. Prof. Hernani Mello 101
24.210-150 Niterói, Brazil
E-mail:
mababinski@gmail.com

Abstract

Introduction: Knowledge of the prostatic portion of the urethra is essential to the comprehension of urinary continence phenomena. However, there are only a small number of studies that have addressed this relationship and analyzed the ultrastructure of the prostatic urethra.
Material and methods: A three-dimensional analysis of the fibrous components and the extracellular matrix of the prostatic urethra in 10 normal humans was performed with a scanning electron microscope. The prostates were obtained from 10 men (18 to 30 years old) who had died from accidents. The specimens were fixated in a modified Karnovsky solution for 48 h at 4°C, washed in a sodium phosphate buffered solution (PBS) for 2 h at 4°C and then incubated in 40 ml of 2 M NaOH at room temperature for 8 days (cellular digestion). Afterwards, the three-dimensional organization of the prostatic urethra stroma was observed.
Results: It was observed that the prostates had a narrowed fibrous septa which condensed and formed a network in order to support the submucosa. Furthermore, it was also observed that they formed a homogeneous fibrous layer (pars fibroreticularis), which lined the urethral wall.
Conclusions: Knowledge of the urethra composition is essential to understand the physiopathological aspects of urinary incontinence. Moreover, our results showed a great amount of connective tissue underlying the prostatic urethra wall.

Key words: prostatic urethra, connective tissue, scanning electron microscopy.

Introduction

The prostatic urethra (PU) is an essential element with respect to the urinary continence physiology. For years its study was neglected in morphological research. McNeal was the first to point out the morphological complexity of the PU and its pathophysiological aspects [1]. Studies showed that the transitional zone (TZ) of the prostate was enlarged in cases of benign prostatic hyperplasia (BPH) [2–5].

Benign prostatic hyperplasia is the most common urologic disorder in elderly men (above 50 years old) [5–7], and it is associated with complex interactions between the epithelial cells [4] and their supportive stroma [3].

Recent studies showed that BPH nodules can cause a significant decrease in elastic fibers and connective tissue of the PU and an increase

AMS

Jorge H.M. Manaia, Gilberto P. Cardoso, Lucas A.S. Pires, Marcio A. Babinski

in fibronectin [8, 9]. Despite this, studies that address the ultrastructural organization of the human PU are scarce [1, 8–10]. Thus, little is known about the ultrastructure of the normal and pathological prostatic urethral wall.

The study conducted herein aims to analyze and elucidate the organization of the extracellular matrix (ECM) of normal human prostates with the aid of a scanning electron microscope (SEM).

Material and methods

Ethical procedures

This study complies with the provisions of the Declaration of Helsinki in 1995 (as revised in Edinburgh, 2000). Our Internal Review Board approved the study guidelines. Also, the protocol was approved by the Ethics Committee on Human Research of the State University of Rio de Janeiro (0040.0.228.000-11).

Samples

Ten prostates were obtained during the autopsy of ten men (mean age: 24 ±4.0 years, range: 18–30) with accidents as causa mortis. The prostates presented normal macroscopic and microscopic aspects (Figure 1). The mean ± SD (range) weight of the gland was 22 ±2.6 g (19.0–25.0). The TZ was located and dissected, as stated by previous studies [1, 2, 4], and the tissue was immediately fixed in a solution of glutaraldehyde (2.5%) and paraformaldehyde (2%) in 0.1 M sodium phosphate buffer (pH 7.4). The time elapsed between death and fixation of the samples was less than 6 h.

Scanning electron microscopy

The specimens were conserved in a modified Karnovsky solution of glutaraldehyde (2.5%) and paraformaldehyde (2%) in 0.1 M sodium phosphate buffer (pH 7.4) for 48 h. Some of the tissue specimens were routinely processed for paraffin embedding and 5 µm thick sections were stained with hematoxylin/eosin and examined by a pathologist not involved in the study to detect and exclude foci of carcinoma or BPH.

To better visualize the three-dimensional organization of the prostatic stroma under the SEM, tissue samples were treated to solubilize and remove cells [9]. Thus, for each man, three fixed TZ fragments (1 × 1 × 0.3 cm) were washed in a sodium phosphate buffered solution (SPBS) for 2 h at 4°C and then incubated in a solution of 2 M NaOH (40 ml) at room temperature for 8 days. During 3 days, the samples were rinsed in a solution containing 40 ml of distilled water at room temperature until they were pale and transparent. This solution was changed during each day of this process.

The processing of materials for high-vacuum SEM followed standard procedures [11]. Decellularized preparations were first treated with 1% tannic acid in an SPBS for 2 h and washed for 1 h. Post-fixation was done in 1% osmium tetro-
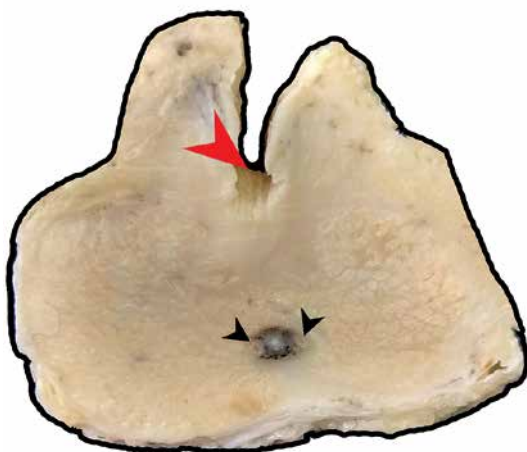
Figure 1. Macroscopic and microscopic aspect of the prostate. The prostatic urethra (PU) is indicated by the red arrowhead. The ejaculatory ducts are also seen (black arrowheads). H&E stain (100×)

xide in an SPBS for 3 h, after which the samples were washed for 1 h and dehydrated in an ascending graded series of ethanol. Samples were then dried with liquid carbon dioxide, mounted on aluminum stubs with carbon cement, and coated with gold using a sputter coater. The samples were examined in an SEM with an acceleration voltage of 15–20 kV.

Measures and photographs of the approximate linear thickness were taken in order to better characterize the fibrous components of the stroma and allow comparison with other tissues. This process was done with the aid of ImageJ 1.37 software. The photographs were taken at 8000× resolution. We also used the same program to extract the mean and standard deviation values. Intact samples (which consisted of fixed but otherwise unprocessed tissue specimens) were also examined directly under low vacuum SEM to assess the luminal surface of the urethral wall and the overall quality of the sample. This SEM technique was also used to monitor the efficiency and extent of the cellular solubilization process.

Results

Decellularized preparations showed that a relatively narrow fibrous septa formed a dense and supportive network for the urethral wall (submucosa layer), as seen in transverse sections (Figure 2).

Removal of the epithelial cells (mucosa) showed a smooth and grossly homogeneous fibrous sheet that lined the surface of the urethral wall. A spongy organization with a thin but dense lamellae delimitated empty spaces on the deeper ECM portion of the fibrous septa. These empty spaces were formerly occupied by cells (Figure 2).

The network of collagen fibers seemed to support the epithelium as a basal layer as seen in a superior view (Figure 3). In this region, the fibers were organized in subjacent parallel layers (formed by collagen fibers arranged in flat bundles). These bundles divided and fused repeatedly, forming a network of collagen fibers which was denser in the basal lamina of the prostatic urethra wall (Figure 2). This smooth sheet consisted of different structural components that formed distinct layers. The superficial layer (beneath the mucosa surface) was smoother and composed of 110–150 nm thick fibrils that grouped parallel to one another and formed a sheet (Figure 3). Under this layer there was a meshwork of loosely woven thin fibrils, with a thickness of 77–115 nm. Those fibrils were oriented in less defined directions (Figure 2).

Discussion

The PU is lined by transitional epithelium. Regional differences may exist and vary from squa-
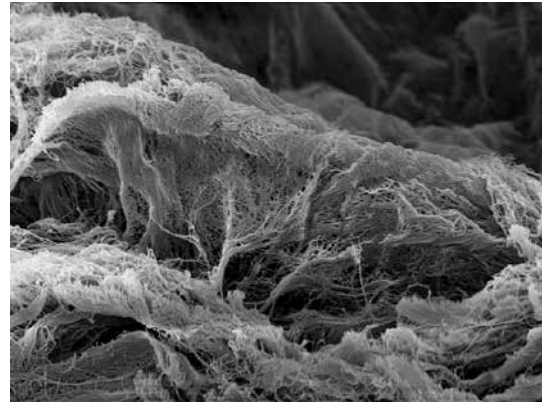
Figure 2. Cross section of the prostatic urethral wall. Smooth and grossly homogeneous fibrous sheet lines with fibrous septa (submucosa) can be seen. Original 8000×
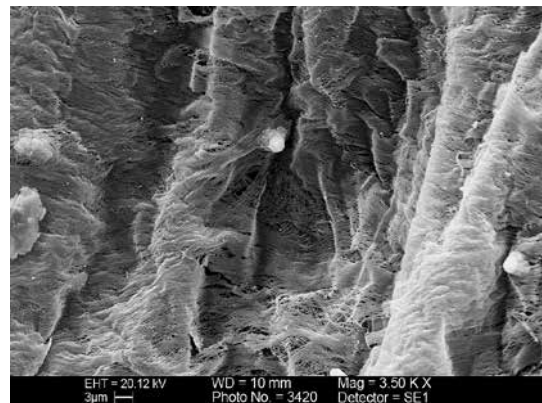
Figure 3. Luminal sheet lining the surface of the empty urethral wall. Higher magnification shows that the luminal sheet is composed of fibrils that possess a parallel arrangement. In places where these fibrils are more widely separated, a meshwork of 110–150-nm thick fibrils forming a layer just underneath can be seen

mous, stratified or pseudostratified columnar epithelium [12, 13]. These variations may extend to the prostatic ducts [14]. It primarily consists of a mucosal layer covered by the urothelium. Beneath the basal membrane lies a layer of connective tissue (submucosa) which contains vascular sinusoids, fibroblasts, an ECM constituted with collagen, proteoglycans, elastic fibers, and glycoproteins [12, 15–17]. Furthermore, the submucosa is composed of an inner longitudinal and an outer circular layer of smooth muscle [14, 18–20]. Recent studies consider the submucosa as a completely independent structure [18–20].

Together, the fibroelastic tissue, collagen and many elastic fibers forms an insoluble ECM that can be found on different organs; moreover, it is reported that their function is to provide elasticity and biomechanical resistance [21].

Thus, elastic fibers and collagen are critical ECM components, with special regard to organs in

Jorge H.M. Manaia, Gilberto P. Cardoso, Lucas A.S. Pires, Marcio A. Babinski

which physiological conditions cause changes in its shape (e.g. the male urethra). These elements of the spongy urethra have been previously studied [15–17, 22].

Studies showed that a significant amount of collagen content was observed through the interaction of elastic fibers with collagen and it was suggested that elastic fibers are important for urethral compliance [22, 23]. The ECM of the PU has received less attention than smooth muscle disposition and innervation; hence, it has not been properly studied [18–20, 24].

A study performed by Lloyd-Davies *et al.* [25] evaluated the urethra and bladder and they proposed that bacterial retention within the urethra and bladder was due to the flow of urine and irregularities of the mucosa. They analyzed the urothelium with the aid of a scanning electron microscope and concluded that urine discharge induced "bacterial washout", as the folds were abolished by distension.

An SEM was used in this study to analyze the three-dimensional organization of the fibrous components in the stroma of the TZ from normal human PU. Our results showed that the PU is structured as a typical membrane composed of three major layers. The first under the epithelium is the lamina lucida, followed by the lamina densa, and lastly there is the poorly delimited pars fibroreticularis [26]. Our results were similar to the findings of a study conducted by Hakky [10], although the author did not evaluate the fibroreticularis framework.

Studies of the tracheal and bronchial basement membranes through an SEM showed that once epithelial cells are gently removed (with EDTA), the lamina densa appears as a homogeneous and smooth sheet [27, 28]. Under this layer there is a more heterogeneous pars fibroreticularis which contains layers of collagen fibers with a variable degree of organization. Our images showed that the stromal component that faces the acinar lumen consists of distinct connective tissue fibrils in a parallel arrangement that is markedly different from the lamina densa morphology, as seen under the SEM.

Therefore, we assume that less resistant components of the lamina densa (such as type IV collagen) were removed by the alkali treatment, which left the pars fibroreticularis exposed. Recent investigations showed that the goal of current processing methods (including decellularization) is to produce a purified ECM, although they rarely resulted in an intact basement membrane [29].

Furthermore, there was a meshwork composed of less organized connective tissue fibers under the luminal fibrous sheet, which should also be part of the pars fibroreticularis, as our results showed. This structural organization was similar to the results of our previous study in prostatic acini [30].

The composition and structure of the pars fibroreticularis are more variable than any other parts of the basement membrane [31] and differences have been found among other tissues, such as rat skin, whereas a less organized meshwork of fibers was immediately followed after the lamina densa [28], or rat trachea, where studies showed that there was firstly a sheet of fibers in a parallel arrangement followed by a layer of fibers with a variable disposition [27].

The latter disposition of pars fibroreticularis was similar to what we found in the human prostate. However, studies showed that the parallel collagen fibers that composed the fibrous sheet under the lamina densa were thicker (average of 500 nm) in the rat tracheas [27], while in the PU, these fibers had a 110–150 nm thickness. This difference might be explained as a functional adaptation, since the prostate acini and ducts are subjected to less stretching forces than the trachea. Previous studies showed that the pars fibroreticularis is structurally more variable than other regions of basement membranes [8].

In conclusion, our results showed that the PU of the normal human prostate presents a dense ECM fibrous component around the urethra and they would act as a diffusion barrier. This barrier might enhance local cellular responses during events that are known to occur in some disorders [8]. The ECM of the prostatic urethral wall also included a distinct pars fibroreticularis, thus supporting the notion of high structural variability in this region regarding the basement membranes.

Acknowledgments

Conflict of interest

The authors declare no conflict of interest.

References

1. McNeal JE. The prostate and prostatic urethra: a morphologic synthesis. J Urol 1972; 107: 1008-16.
2. McNeal JE. Anatomy of the prostate and morphogenesis of BPH. Prog Clin Biol Res 1984; 145: 27-53.
3. Chagas MA, Babinski MA, Costa WS, Sampaio FJB. Stromal and acinar components of the transition zone in normal and hyperplastic human prostate. BJU Int 2002; 89: 699-702.
4. Babinski MA, Chagas MA, Costa WS, Sampaio FJB. Prostatic epithelial and luminal area in the transition zone acini: morphometric analysis in normal and hyperplastic human prostate. BJU Int 2003; 92: 592-6.
5. Wei JT, Calhoun E, Jacobsen SJ. Urologic diseases in America project: benign prostatic hyperplasia. J Urol 2005; 173: 1256-61.

6. McNeal JE. Prostate. In: Histology for Pathologists. Sterenberg SS (ed.). Lippincott-Raven, Philadelphia 1997; 997-1017.

7. Prajsner A, Chudek J, Szybalska A, et al. Socioeconomic determinants of prostate-specific antigen testing and estimation of the prevalence of undiagnosed prostate cancer in an elderly Polish population based on the Pol-Senior study. Arch Med Sci 2016; 12: 1028-35.

8. Babinski MA, Manaia JHM, Cardoso GP, Costa WS, Sampaio FJB. Significant decrease of extracellular matrix in prostatic urethra of patients with benign prostatic hyperplasia. Histol Histopathol 2014; 29: 57-63.

9. Manaia JHM, Cardoso GP, Babinski MA. Stereological evaluation of fibronectin in the periurethral region of the transitional zone from normal human prostates compared with benign prostatic hyperplasia. Int J Clin Exp Pathol 2015; 8: 4143-7.

10. Hakky SI. Ultrastructure of the normal human urethra. Br J Urol 1979; 51: 304-7.

11. Ohtani O. Three-dimensional organization of the collagen fibrilar framework of the human and rat livers. Arch Histol Cytol 1988; 51: 473-88.

12. Tanagho EA, McAninch JW. Smith's General Urology. McGraw-Hill, New York 2000.

13. Orlandini GE, Orlandini SZ, Holstein AF, Evangelisti R, Ponchietti R. Scanning electron microscopic observations on the epithelium of the human prostatic urethra. Andrologia 1987; 19: 315-21.

14. Roehrborn CG, McConnell JD. Etiology, pathophysiology, epidemiology and natural history of benign prostatic hyperplasia. In: Campbell's Urology. Walsh PC, Retik AB, Vaughan Jr ED, Wein AJ (eds.). WB Saunders, Philadelphia 2002.

15. Da-Silva EA, Sampaio FJB, Dornas MC, Damião R, Cardoso LEM. Extracellular matrix changes in urethral stricture disease. J Urol 2002; 168: 805-7.

16. Da-Silva EA, Sampaio FJB, Ortiz V, Cardoso LEM. Regional differences in the extracellular matrix of the human spongy urethra as evidenced by the composition of glycosaminoglycans. J Urol 2002; 167: 2183-7.

17. Bastos AL, Da-Silva EA, Costa WS, Sampaio FJB. The concentration of elastic fibres in the male urethra during human fetal development. BJU Int 2004; 94: 620-3.

18. Dorschner W, Stolzenburg JU, Neuhaus J. Structure and function of the bladder neck. Adv Anat Embryol Cell Biol 2001; 159: 1-13.

19. Stolzenburg JU, Schwalenberg T, Dorschner W, Salomon FV, Jurina K, Neuhaus J. Is the male dog comparable to human? A histological study of the muscle systems of the lower urinary tract. Anat Histol Embryol 2002; 31: 198-205.

20. Yucel S, Baskin LS. An anatomical description of the male and female urethral sphincter complex. J Urol 2004; 17: 1890-7.

21. Kielty CM, Sherrat MJ, Shuttleworth CA. Elastic fibers. J Cell Sci 2002; 115: 2817-28.

22. Baskin LS, Constantinescu SC, Howard PS, et al. Biochemical characterization and quantitation of collagenous components of urethral stricture tissue. J Urol 1993; 150: 642-7.

23. Singh M, Blandy JP. The pathology of urethral stricture. J Urol 1976; 115: 673-6.

24. Karam I, Moudouni S, Droupy S, Abd-Alsamad I, Uhl JF, Delmas V. The structure and innervation of the male urethra: histological and immunohistochemical studies with three dimensional reconstruction. J Anat 2005; 206: 395-403.

25. Lloyd-Davies RW, Hayes TL, Hinman F. Urothelial microcontour. I. Scanning electron microscopy of normal resting and stretched urethra and bladder. J Urol 1971; 105: 236-41.

26. Lindblom A, Paulsson M. Basement membranes. In: Extracellular Matrix. Comper WD (ed.). Harwood Academic Publishers, The Netherlands 1996; 132-63.

27. Evans MJ, Van Winkle LS, Fanucchi MV, et al. Three-dimensional organization of the lamina reticularis in the rat tracheal basement membrane zone. Am J Respir Cell Mol Biol 2000; 22: 393-7.

28. Osawa T, Feng XY, Nozaka Y. Scanning electron microscopic observations of the basement membranes with dithiothreitol separation. Med Electron Microsc 2003; 36: 132-8.

29. Brown B, LIndberg K, Reing J, Stoiz DB, Badylak SF. The basement membrane component of biologic scaffolds derived from extracellular matrix. Tissue Eng 2006; 12: 519-26.

30. Babinski MA, Costa WS, Sampaio FJ, Cardoso LE. Structural organization of fibrous connective tissue in the periacinar region of the transitional zone from normal human prostates as revealed by scanning electron microscopy. BJU Int 2007; 100: 940-4.

31. Merker HJ. Morphology of the basement membrane. Microsc Res Tech 1994; 28: 95-124.